Alpha-synuclein pathology, microgliosis, and parvalbumin neuron loss in the amygdala associated with enhanced fear in the Thy1-aSyn model of Parkinson's disease

Eileen Ruth S. Torres[1,*], **Milos Stanojlovic**[5,*], **Moriel Zelikowsky**[2,4,**], **Jana Bonsberger**[5], **Sindalana Hean**[1], **Caitlin Mulligan**[1], **Leonie Baldauf**[5], **Sheila Fleming**[1], **Eliezer Masliah**[3], **Marie-Francoise Chesselet**[1], **Michael S. Fanselow**[2], **Franziska Richter**[1,5,6,**]

[1]Department of Neurology, The David Geffen School of Medicine at UCLA, Los Angeles, CA 90095, USA

[2]Department of Psychology, Staglin Center for Brain and Behavioral Health, UCLA, Los Angeles, CA 90095, USA

[3]Department of Neurosciences, UCSD School of Medicine, La Jolla, CA 92093, USA

[4]Department of Biology and Biological Engineering, California Institute of Technology, Pasadena, CA 91125, USA

[5]Department of Pharmacology, Toxicology and Pharmacy, University of Veterinary Medicine Hannover, 30559 Hannover, Germany

[6]Center for Systems Neuroscience, Hanover, Germany

Abstract

In Parkinson's disease (PD), the second most common neurodegenerative disorder, non-motor symptoms often precede the development of debilitating motor symptoms and present a severe impact on the quality of life. Lewy bodies containing misfolded α-synuclein progressively develop in neurons throughout the peripheral and central nervous system, which may be correlated with the early development of non-motor symptoms. Among those, increased fear and anxiety is frequent in PD and thought to result from pathology outside the dopaminergic system, which has been the focus of symptomatic treatment to alleviate motor symptoms. Alpha-synuclein accumulation has

Co-Corresponding Authors: Franziska Richter DVM, Ph.D., Department of Pharmacology, Toxicology and Pharmacy, University of Veterinary Medicine Hannover, Foundation, Bünteweg 17, 30559 Hannover, Germany, franziska.richter@tiho-hannover.de, Moriel Zelikowsky, Ph.D., Department of Neurobiology, University of Utah, 20 S 2030 E, Salt Lake City UT 84112, moriel.zelikowsky@neuro.utah.edu.
*contributed equally

been reported in the amygdala of PD patients, a brain region critically involved in fear and anxiety. Here we asked whether α-synuclein overexpression alone is sufficient to induce an enhanced fear phenotype in vivo and which pathological mechanisms are involved. Transgenic mice expressing human wild-type α-synuclein (Thy1-aSyn), a well-established model of PD, were subjected to fear conditioning followed by extinction and then tested for extinction memory retention followed by histopathological analysis. Thy1-aSyn mice showed enhanced tone fear across acquisition and extinction compared to wild-type littermates, as well as a trend to less retention of fear extinction. Immunohistochemical analysis of the basolateral nucleus of the amygdala, a nucleus critically involved in tone fear learning, revealed extensive α-synuclein pathology, with accumulation, phosphorylation, and aggregation of α-synuclein in transgenic mice. This pathology was accompanied by microgliosis and parvalbumin neuron loss in this nucleus, which could explain the enhanced fear phenotype. Importantly, this non-motor phenotype was detected in the pre-clinical phase, prior to dopamine loss in Thy1-aSyn mice, thus replicating observations in patients. Results obtained in this study suggest a possible mechanism by which increased anxiety and maladaptive fear processing may occur in PD, opening a door for therapeutic options and further early biomarker research.

Introduction

Parkinson's Disease (PD), the second most common neurodegenerative disorder is affecting 1–2‰ of the global population (Tysnes and Storstein, 2017). PD is identified as the fastest growing neurological disease in terms of prevalence, disability, and deaths (GBD 2015 Neurological Disorders Collaborator Group, 2017), and estimates are that the number of PD patients is going to double in the next 30 years (Rocca, 2018). Hallmarks of PD are appearance of Lewy bodies, aggregates of misfolded protein, and dopaminergic neuronal loss in the *substantia nigra pars compacta* which lead to the characteristic motor symptoms (Poewe et al., 2017). Importantly, PD is also associated with a plethora of non-motor symptoms, cognitive and sleep impairment, abnormalities in sensation and autonomic function and mood disorders, some of which appear before the characteristic motor symptoms (Pfeiffer, 2016).

Mood disorders and emotional disturbances are frequent in PD patients and thought to result from extra-nigral pathology, explaining the resistance to dopaminergic treatments (Connolly and Fox, 2014; Duncan et al., 2014; Mufti and LaFaver, 2020; Rahman et al., 2014; Yamanishi et al., 2013). Anxiety typically presents before the classical motor symptoms lead to PD diagnosis, suggesting an early neuropathological process (Chen and Marsh, 2014; Schrag and Taddei, 2017).

The amygdala plays a key role in fear and anxiety (Ressler, 2010; Steimer, 2002). Abnormal accumulation of the main Lewy body protein component, α-synuclein (α-syn), has been found post-mortem in the amygdala of patients with PD and other synucleinopathies

(Bertrand et al., 2004; Dickson et al., 2009; Sorrentino et al., 2019) and may occur early during disease progression (Braak et al., 2003). This suggests a possible role for the amygdala in PD anxiety disorders. Inhibitory GABA-ergic fast-spiking interneurons that express the Ca^{2+} binding protein, parvalbumin, are distributed throughout the brain including the amygdala and play important roles in synaptic plasticity, anxiety, social interaction and memory extinction (Villalobos et al., 2018) (Caillard et al., 2000; Zou et al., 2016). Interestingly, parvalbumin neuron-specific α-syn accumulations have been detected in the amygdala of PD patients, suggesting differential vulnerability of parvalbumin neurons to α-syn-associated pathology (Flores-Cuadrado et al., 2017). Together with parvalbumin positive interneurons, interneurons expressing calbindin D28K (calbindin) are involved in the regulation of fear responses and anxiety (Krabbe et al., 2018; Wolff et al., 2014). Both, parvalbumin and calbindin play a crucial role in Ca^{2+} buffering and regulation of Ca^{2+} signaling, processes that are both affected in PD (Foehring et al., 2009; Surmeier et al., 2017; Zaichick et al., 2017).

Previous studies showed that transgenic mouse models expressing mutated α-syn (A53T, A30P) have reduced anxiety-like behavior and decreased freezing behavior (Freichel et al., 2007; George et al., 2008; Stanojlovic et al., 2019a), supporting the notion that α-syn pathology interferes with anxiety-related behaviors; however, increased anxiety as seen in PD patients was not observed. In this study, we used a PD mouse model in which the pan-neuronal Thy-1 promoter (Thy1-aSyn) regulates expression of human wild-type α-syn (Chesselet et al., 2012). Human wild-type α-syn overexpression throughout the brain generates progressive formation of proteinase K-resistant α-syn aggregates in cell bodies and neurites in this model, that are observed in several brain regions including the substantia nigra (Chesselet et al., 2012; Fernagut et al., 2007). In addition to early and progressive sensorimotor impairments and striatal dopamine loss, these mice show several early non-motor symptoms including olfactory, autonomic, gastrointestinal, sleep and cognitive deficits (Chesselet et al., 2012; Fleming et al., 2008; McDowell et al., 2014; Morris et al., 2015; Wang et al., 2012). This prompted us to investigate fear-related behaviors in Thy1-aSyn mice at early stages of progression and underlying pathological mechanisms in the amygdala.

Materials and Methods

1. Animals

Transgenic mice overexpressing human wild-type α-syn under the Thy-1 promoter (Rockenstein et al., 2002) are maintained on a mixed C57BL/6-DBA/2 background as described previously (Chesselet et al., 2012). Polymerase chain reaction (PCR) amplification analysis of tail samples was performed on tissue samples collected both at birth and at the completion of each experiment, and only animals with confirmed genotypes were included in statistical analysis. All animals were treated in accordance with the United States Public Health Service Guide for the Care and Use of Laboratory Animals with all procedures approved by the Institutional Animal Care and Use Committee at the University of California Los Angeles, or according to the EU council directive 2010/63/EU and the German Law on Animal Protection with approvals for breeding and the procedures by

the respective government agency (Lower Saxony State Office for Consumer Protection and Food Safety). All efforts were made to minimize both the suffering and the number of animals. All animal experiments of this study were conducted and are reported in accordance with ARRIVE guidelines.

Only male transgenic mice were used along with wild-type littermates. Due to the location of the transgene on the X-chromosome, female Thy1-aSyn mice show no or subtle phenotypes in most behavioral assays (Chesselet et al., 2012; Gerstenberger et al., 2016). Littermates of the same sex were housed together at a maximum occupancy of four mice per cage under specific pathogen free conditions in open lid cages. Animals were maintained on a reverse 12 hour dark/light cycle, and food (standard rodent chow) and water were available *ad libitum*. Except for the stress-induced hyperthermia test, all testing was done during the dark cycle when mice are most active at low light. Mice were habituated to the room prior to behavioral testing, and light and noise levels kept constant. Sample sizes were determined based on *a priori* power analysis. For the fear conditioning part of this study, experimental groups included n=11 Thy1-aSyn and n=10 wild-type littermates at 3–4 months of age. Following fear-condition and the flinch-jump-vocalization test, n=5 wild-type and n=9 Thy1-aSyn transgenic mice were randomly chosen for stress-induced hyperthermia and pain sensitivity testing using the hot plate test. For histology mice at 5–6 months of age were used, which consisted of randomly chosen n=6 wild-type and n=4 Thy1-aSyn transgenics from the fear-conditioned mice and a further batch of n=6/genotype which had not undergone behavioral testing.

2. Fear Conditioning

Apparatus—Mice were conditioned and tested in groups of four using four identical conditioned chambers (30 X 25 X 25 cm, Med-Associates, Inc St. Albans, VT), which were equipped with a Med-Associates VideoFreeze system. Each chamber consisted of Plexiglass front doors, back walls, and ceilings with aluminum side walls; individual boxes were enclosed within sound-attenuating chambers. A stainless steel pan was placed underneath and sprayed with an odorant. Two physical contexts, A and B, were used throughout fear conditioning and extinction trials in order to provide two unique environments differentiated by chamber-shape, illumination, odor, cleaning solution, and background noise. Each set of context boxes was placed in a dedicated experimental room in order to provide a unique spatial location.

Context A was characterized by a single lined floor grid consisting of 16 stainless steel rods (4.8 mm thick) each spaced 1.6 cm apart (center to center) (Med-Associates, Inc.) and a blue dot pattern on the back wall. The floor pans were sprayed with Simple Green® as a scent. Each chamber was cleaned with 70 % isopropyl alcohol between squads. Fans in each chamber were turned on to create background noise (60 dB).

In Context B, the floor was made up of two planes of staggered stainless steel rods (4.8 mm thick) spaced 1.6 cm apart (center to center) (Med-Associates, Inc). The rear wall was white and opaque and a black plastic insert provided sidewalls to create a triangular roof. Context B chambers were scented and cleaned with 1 % acetic acid solution, and the fan was left off.

Data Analyses—Activity and freezing were recorded using an automated near infrared video tracking equipment and computer software (VideoFreeze; Med-Associates Inc.) as described previously (Cushman et al., 2011). Using a video recorded at 30 frames per second, the software calculated the noise (standard deviation) for each pixel in a frame by comparing its grayscale value to previous and subsequent frames, producing an "activity unit" score for each frame. Freezing was defined as subthreshold activity (set at 19 activity units) for longer than 1 second, which was validated by a human observer previously. The first 3 seconds of the 30-second post-shock interval were not analyzed for freezing behavior as the animals show an activity burst in response to the shock during this period (Fanselow, 1982).

Procedure—The two days prior to the first day of conditioning, animals were placed in a holding room adjacent to the testing room for one to two hours during their light cycle for habituation. On the second day of habituation, tails were marked to ensure proper identification in addition to earmarks. Mice were habituated for an hour in the holding room each day before testing. Figure 1 summarizes the fear conditioning procedure.

Fear acquisition took place in Context A (Day 1). Squads of four, which were counterbalanced across genotype, were tested at a time. Acquisition began with a three minute "baseline" (BL) period to allow acclimation to the experimental chamber. This was followed by 3 conditioning trials in which 20 s presentations of a tone co-terminated with a 2 s footshock (0.6 mA). The inter-trial interval (ITI) was 3 minutes. The next day (Day 2), mice were placed back into Context A for an eight minute context fear test. Mice were then pre-exposed to the novel context B for 8 minutes (Day 3) before being tested for tone fear in context B (Day 4) with the same protocol as acquisition, but with the shocks omitted.

One month later, mice were extinguished in context B. Extinction training consisted of a 3 min baseline followed by 15, 20 s tone presentations separated by a 60 s inter-trial interval (ITI). An identical extinction session was repeated the following day to ensure that freezing levels were adequately reduced. Following successful extinction of freezing behavior, a number of mice demonstrated periods of time (towards the end of our long extinction sessions) with relatively little movement, consistent with potential sleep behavior. Mice were then divided into two counterbalanced groups to test for tone extinction memory in context B (extinction retention) or tone fear renewal in Context A (fear renewal). Half of the animals received renewal testing first and then extinction retention; the second half received tests in the opposite order. Tone tests included a three-minute baseline followed by three tones separated by a 60 sec ITI.

Measurement of Crossover Activity During Baseline Period—Crossover activity during the baseline periods in each context prior to any tone or shock administration for the initial four days (acquisition, context test, pre-exposure to context B, tone test) was assessed manually by an observer blind to genotypes. The video was manually scored for crossovers, defined as the animal crossing the midline with all 4 paws (Cushman et al., 2011).

3. Pain Sensitivity and Stress Tests

To ensure that differences in fear responses were not due to a difference in pain sensitivity or stress response, mice were tested for heightened pain sensitivity and stress response using three different methods.

Flinch-Jump-Vocalization Test—For the pain perception test, or Flinch-Jump-Vocalization (Flinch-Jump) Test (De Oca et al., 1998), each mouse was placed into a fear conditioning chamber equipped with a shock generator. Beginning with an intensity of 0.0 mA, the intensity of the 2 second-shock was increased by 0.05 mA at equal time intervals of 10 seconds. An observer blind to the animals' genotypes noted at what intensity the animal flinched, jumped, and vocalized in response to the shock. This was repeated three times for each animal. Flinching was defined as lifting a forepaw, jumping was marked as when all four paws were off the ground, and vocalization was when the mouse vocalization was audible to the observer.

Hot Plate Test—As an additional measure of pain sensitivity, mice were tested using a hot plate test. Mice were brought to the testing room in the morning and habituated the entire day until the dark cycle. The hot plate was heated to 55°C for at least 10 minutes and was measured throughout the test to maintain the temperature within 0.2°C. A clear, plastic cylinder was placed on top of the hot plate to contain the animals. Mice were then placed onto the hot plate individually, and the time taken for the mouse to lick its paw (seconds) was recorded.

Stress-Induced Hyperthermia Test—Stress-induced hyperthermia (SIH) has been previously validated as a method to measure anxiety in mice (Olivier et al., 2003). It was performed for this study as a measure of how mice react to stimuli. Groups of both Thy1-aSyn (n = 9) and wild-type (n = 5) mice were brought to the testing room and singly housed in new, clean cages the evening prior to the test one hour before lights off. Testing occurred two hours after lights were turned on in the morning. The baseline core temperature for each mouse was recorded by scruffing the animal—a novel, stressful experience—and using a rectal thermometer lightly lubricated with petroleum jelly and disinfected with 70 % isopropyl alcohol between each mouse. Approximately ten minutes after the initial baseline was taken, a second temperature was taken. In order to maintain a ten-minute time interval between the baseline and second temperatures, the mice were tested in two batches of 8 and 6 each. All mice were tested by alternating Thy1-aSyn and wild-type mice. The differences between the baseline and second temperatures were calculated and used for analysis.

4. Immunohistochemistry

For immunohistochemical analysis of α-syn pathology, 5–6-month old wild-type and Thy1-aSyn male mice were selected randomly from mice that had undergone behavioral testing (n=6 wild-type, n=4 Thy1-aSyn transgenics) and perfused transcardially with 4 % paraformaldehyde. The brains were removed, post-fixed in 4 % paraformaldehyde, cryoprotected in 30 % sucrose in 0.1M PBS over 24 hours, and frozen on dry ice. Brains were then cut into coronal sections (40 μm) on a cryostat and sections through the amygdala were collected and assessed for immunohistochemistry.

For α-syn expression analysis two adjacent coronal sections from the center of the basal lateral nucleus of the amygdala were chosen based on the anatomical atlas by Paxinos and Franklin (Paxinos and Franklin, 2004). One of these two sections from each mouse was stained for Nissl and used as a reference section to confirm anatomical landmarks. The second section for each mouse was washed with 0.05 M TBS for ten minutes three times and then treated with M.O.M. blocking reagent (Vector Lab, PK-2200) followed by 10 % NGS in TBS. Then, sections were incubated overnight in 2 % NGS/0.5 % TritonX in TBS with a primary antibody that recognizes both mouse and human α-syn (van der Putten et al., 2000), mouse anti-α-syn (clone 42, mouse mAb raised against rat α-syn (aa 15–123), 1:500, BD Biosciences, San Jose, CA) and with a primary antibody that recognizes α-syn only when it is phosphorylated at serine 129 (1:250, Abcam #59264). Following incubation with primary antibodies, sections were washed with 0.05M TBS three times for ten minutes each wash and then incubated in 1:500 dilution of Goat anti Rabbit IgG Cy3 (Millipore) and Goat anti Mouse IgG Dylight 649 (Jackson Immunoresearch) in 5 % NGS for two hours. After another round of washing, the sections were mounted on plain slides and scanned for immunoreactivity using an Agilent microarray scanner equipped with a krypton/argon laser (647 nm) at 10 μm resolution with the photomultiplier tube (PMT) set at 5 %. ImageJ (National Institutes of Health) was used to quantify the immunofluorescence intensity of the staining in the amygdala (Lu et al., 2009). Finally, sections were covered using Vectashield mounting medium for fluorescence (Vector Laboratories) and scanned using a Leica TCS SP5 MP-STED confocal microscope to further analyze α-syn staining and colocalization of total and phosphorylated α-syn. For visualization of α-syn aggregates, sections were processed as described above for α-syn immunoreactivity, but prior to incubation with the same primary antibody, sections were incubated at room temperature for 10 minutes in 0.1 M PBS containing 10 μg/ml of Proteinase K (Invitrogen, Carlsbad, CA) and then washed with 0.1 M PBS. After incubation in primary antibody, sections were washed in 0.1 M PBS followed by a 2-hour incubation with a biotinylated goat anti-mouse IgG F(ab')2 (Jackson ImmunoResearch) at room temperature in the presence of 2 % normal goat serum, washed in 0.1 M PBS and incubated in avidin-biotin complex (ABC; Vector Laboratories) for 45 minutes and rinsed again in 0.1 M PBS followed by an incubation in 0.05 M TBS pH 7.6 containing 0.03 % DAB and 0.3 % H2O2 to reveal staining. After a final rinse in 0.1 M PBS sections were mounted on charged glass slides, dehydrated, cleared with xylene, and mounted with Eukit mounting medium (Calibrated Instruments, Hawthorne, NY). Sections were examined under bright-field illumination with a Zeiss Axioskop microscope (Thornwood, NY) and digital images were captured by a Spot digital camera (Sterling Heights, MI).

For parvalbumin, calbindin, NeuN, c-Fos, IBA1 and phosphorylated α-syn co-localization analysis a second batch of 6 months old naive wild-type and Thy1-aSyn male mice (n=6/ group) was processed as described above. Brains were then cut into coronal sections (40 μm) and every 6th section from bregma −0.58 to bregma −1.82 (Paxinos and Franklin, 2004) (total of 5) through the amygdala collected. The sections were washed with 0.05M TBS for ten minutes three times and were blocked using 10 % NGS in TBS. Then, sections were incubated overnight in 2 % NGS/0.5 % TritonX in TBS with a primary antibodies (guinea pig anti-parvalbumin, 1:500, Synaptic Systems, Göttingen, DE; rabbit anti-calbindin,

1:500, Synaptic Systems, Göttingen, DE; mouse anti-GAD65/67, 1:500 MerckMillipore, Burlington, MA; rabbit anti IBA1, 1:500, Synaptic Systems, Göttingen, DE; mouse anti-NeuN, 1:500 MerckMilipore, Burlington, MA; mouse Serine 129 phosphorylated α-syn, 1:500 Abcam, Cambridge, rabbit c-Fos, 1:500 Synaptic Systems, Göttingen, DE). Sections were washed with 0.05 M TBS three times for ten minutes each wash and then incubated in 1:500 dilution of Alexa Fluor® goat anti-guinea pig 647, Alexa Fluor® goat anti-rabbit 488, and Alexa Fluor® goat anti-mouse 555 (1:500, MerckMilipore, Burlington, MA) 5 % NGS for two hours. After another round of washing, sections were mounted on glass slides and covered with ProLong®Gold with DAPI (Cell Signaling, Danvers, MA). ZEISS Axio Observer microscope and Zen Zeiss software (Oberkochen, DE) was used to capture low (10×) and higher (20×) magnification images. Higher magnification images were analyzed using ImageJ software. Every 6th section from bregma −0.58 to bregma −1.82 (Paxinos and Franklin, 2004) (total of 5) from wild-type and Thy1-aSyn mice (n=6/group) containing BLA was analyzed; Parvalbumin positive cells were considered only if they met the morphological criteria (neuronal shape) and if a nucleus was present (DAPI staining). Cell density was obtained by dividing the number of counted cells by the BLA area. High magnification images (63×, oil immersion) were obtained using ZEISS Apotome to demonstrate co-localization (Oberkochen, DE).

Statistics—Automated near infrared (NIR) video tracking equipment and computer software (Videofreeze, Med-Associates Inc.) was used to record all behavior during fear conditioning/testing. Video was recorded at 30 frames per second; an "activity unit" for each frame was produced by the software calculating the noise (standard deviation) for each pixel in a frame and comparing its grayscale value to previous and subsequent frames. Average freezing was rated for all behavioral testing days for baseline periods, during each tone, as well as during ITIs. For extinction learning, tone presentations were grouped into blocks of 5 as "bins" to aid in presentation. All data passed the normality test (Shapiro-Wilk). Two-way repeated measures ANOVA followed by Fisher's LSD post hoc was used to assess fear conditioning data, and Student's t-test to for the hot plate test and stress-induced hyperthermia. For immunohistochemistry Student's t-test was used to compare immunoreactivity in wild-type versus Thy1-aSyn mice. Frequencies were compared with fisher exact test. The significance level was set at p < 0.05 for all analyses. Grubbs test was used to determine outliers (p < 0.05). All statistics were calculated using GraphPad Prism (GraphPad Software, Inc., San Diego, CA, USA, 2003) and SigmaPlot 12.0 (Systat Software, Inc., San Jose, CA).

Results

Mice overexpressing α-syn show enhanced tone fear

Animals were exposed to tone fear conditioning, tested, submitted to extinction, and tested for extinction memory (diagram of behavioral analyses in Figure 1). During fear acquisition, no significant differences in freezing between genotypes were seen during the baseline, tone, or inter-trial interval (ITI) periods (p>0.05). The following day (context test), a repeated measures ANOVA did not reveal any genotype differences (main genotype effect F1/133=0.321 p=0.578), indicating that mice froze to the context similarly across genotype

condition (Figure 2A). On day 3 (pre-exposure to context B), no differences in freezing were seen (not shown). The following day (tone test), Thy1-aSyn mice showed a trend to increased average tone freezing compared to wild-type (p=0.088, student's t-test, Fig. 2B) and a significant shift in distribution towards higher freezing (p=0.035, fisher exact test on 2×2 contingency table separating mice with more or less than 30 % average freezing, Fig. 2C). When tone freezing was broken down into each of the three tones, Thy1-aSyn mice displayed enhanced freezing in response to the final tone presentation, when compared to wild-type controls (p=0.01, Fisher's LSD following ANOVA; Fig. 2D).

Enhanced fear response in Thy1-aSyn mice persisted during extinction and retention

During extinction training in context B, the enhanced tone fear in Thy1-aSyn mice compared to wild-type mice persisted. Both genotypes showed significant within-session extinction (main effect of trial F1/323=4.186 p<0.001), although wild-type mice reached baseline levels by the third tone, while it took Thy1-aSyn mice 8 tones (Fig. 3A). At tone 1 (p=0.046), 6 (p=0.02), 7 (p=0.025), and 9 (p=0.048) Thy1-aSyn mice showed enhanced freezing (Fisher's LSD following ANOVA, Fig. 3A).

The extinction retention test in context B and fear renewal test in context A showed no significant differences between genotypes or between renewal versus extinction tests when freezing was collapsed across tones (2X2 RM ANOVA, p>0.05) (Fig. 3B). However, Thy1-aSyn mice exhibited a strong trend to an increase in fear response when genotypes were compared across tests during the final tone presentation (Student's t-test with Welch's correction, p=0.0538). In summary, the overall enhanced fear in Thy1-aSyn mice persisted following extinction, despite intact within-session tone fear extinction, suggesting that what was learned during extinction was also less retained by Thy1-aSyn mice.

Increased fear response in Thy1-aSyn mice is not due to enhanced stress or pain sensitivity

Enhanced acquisition of fear due to increased responsiveness to stress or pain could be responsible for increased fear responses in Thy1-aSyn mice. We therefore performed a battery of tests to describe the response of these mice to foot shock, to pain, and to stress (Fig. 4).

Activity bursts, latency to resume freezing, and the flinch-jump vocalization test characterize the animals' responsiveness to shock (Fig. 4A-D). Thy1-aSyn mice showed an increase in activity burst after the third of the three foot shocks applied during acquisition (2X3 RM ANOVA main effect of genotype F1/38=4.642 p=0.044; main effect of trial F2/38=2.062 p=0.141; wild-type versus Thy1-aSyn on trial 3 p=0.011 Fisher's LSD, Fig. 4A). When data for the latency to resume freezing after the shock was assessed, there was a significant genotype x time interaction (F2/38=5.784 p=0.006). Thy1-aSyn mice took significantly less time to resume freezing after receiving the first shock (Fisher's LSD, p=0.008, Fig. 4B). To further test for a difference in pain sensitivity, we used the flinch-jump-vocalization test to measure the threshold of shock intensity (mA) at which mice flinch (low level), jump (medium level), and vocalize (high level) (Fig. 4C). Thy1-aSyn mice and wild-type mice flinched at the same low level of shock intensity, supporting similar sensitivity.

Further, both genotypes vocalized when foot shock was perceived as painful around the same shock intensity. Interestingly, Thy1-aSyn mice seemed to respond with jumps at a lower shock level, indicating a decreased threshold for this behavior which could be related to the increased strength in activity bursting seen during acquisition (2X3 RM ANOVA, main effect of test flinch/jump/vocalize F2/36=23.803 p<0.001; main effect of genotype F1/36=1.265 p=0.274; Fisher's LSD p=0.037 for jump wild-type versus Thy1-aSyn). To further test whether Thy1-aSyn mice are more pain sensitive, we used the hot plate test. Time to lick paw in response to a heated plate was recorded for each mouse (Figure 4D). Student's t-test showed no significant difference in average times between genotypes supporting that Thy1-aSyn mice do not exhibit a greater sensitivity to pain. Hence, the increase in jump response and activity bursts upon foot shocks may be related to the hyperactivity phenotype and increase of extracellular striatal dopamine that becomes apparent at 5–6 months of age (Lam et al. 2011).

In order to rule out that an increased response to stress could have accounted for the increased fear response in Thy1-aSyn mice, we measured stress-induced hyperthermia. All mice except one showed an increase in internal temperature; this animal was not found to be an outlier (Grubbs test). Student's t-test showed no significant difference between the mean temperature change of each genotype (Figure 4E) supporting similar stress responses in Thy1-aSyn mice compared to wild-type.

Thy1-aSyn mice did not show differences in general activity during fear conditioning

Thy1-aSyn mice at 6 months of age show hyperactivity if placed for 15 minutes in an open field (Lam et al., 2011). While mice in this study were 3–4 months old and less likely to exhibit hyperactivity, we ensured that this phenotype did not interfere with fear learning and freezing. Therefore, we assessed crossover activity, a measurement of activity levels, during the three-minute baseline periods of the different testing days. A 2X3 RM ANOVA revealed no difference between genotypes in crossover activity for all testing days (data shown in Fig. 5 for day 1, acquisition in context A, and day 4, tone test in context B).

Alpha-syn pathology in the amygdala of Thy1-aSyn mice

The amygdala has been implicated in emotional abnormalities and pathological α-syn aggregates are observed in the amygdala of PD patients. Therefore we sought to determine whether α-syn overexpression, pathological aggregates, and phosphorylation at serine 129 were present in the amygdala of the Thy1-aSyn mice. Phosphorylated α-syn accumulates in PD brains and in Thy1-aSyn mice (Lee et al., 2011). Representative images taken with a high resolution scanner of sections double-labeled for mouse/human α-syn and phosphorylated α-syn are shown in Figure 6. The BLA exhibits overt staining in transgenic mice compared to wild-type (Fig. 6A). Immunofluorescence intensity was quantified using ImageJ. Thy1-aSyn exhibited increased expression of α-syn detected with an antibody that recognizes both human and mouse α-syn and increased levels of phosphorylated α-syn in the amygdala (p=0.028, Student's t-test, Fig. 6B). In order to determine with greater precision in which region and cell types of the amygdala α-syn accumulated in Thy1-aSyn mice, sections were then examined using high magnification microscopy and apotome. Alpha-syn accumulation and phosphorylation were particularly intense in the BLA, whereby

phosphorylated α-syn accumulated preferably in NeuN positive cells specifically in the BLA (Fig. 6C,D). IBA-1 positive microglia cells were prominent in the BLA and appeared with enlarged cell bodies and prominent processes indicative of activation. Quantification of phosphorylated α-syn from these images confirmed accumulation in Thy1-aSyn mice at 6 months (p=0.001, Student's t-test), which was still present at 16 months of age (p=0.046, Student's t-test, Fig. 6E, F).

In PD, α-syn is present in insoluble protein aggregates (Spillantini et al., 1997). In Thy1-aSyn mice accumulation of α-syn results in the formation of proteinase K-resistant aggregates in some regions of the brain, including the substantia nigra (Fernagut et al., 2007). Aggregation of α-syn had not been previously assessed in the amygdala in this model. Here we show that α-syn accumulation in the BLA results in the formation of proteinase K-resistant aggregates (Fig. 7).

Microglial activation and parvalbumin positive neuron loss in the amygdala of Thy1-aSyn mice

Neuroinflammation is considered an important contributing factor to PD pathology, likely related to α-syn, and observed in the striatum and substantia nigra of Thy1-aSyn mice (Allen Reish and Standaert, 2015; Watson et al., 2012). Proteinase K-resistant aggregates and increased levels of phosphorylated α-syn in the BLA prompted us to investigate neuroinflammatory processes by examining IBA1-positive microglia (Fig. 8). NeuN was used as a neuronal marker to delineate the BLA. Similar to previous quantifications in the striatum and substantia nigra (Watson et al., 2012), microglia appeared larger with more prominent processes in the BLA of Thy1-aSyn mice than in wild-type mice, indicative of microglial activation (Fig. 8D3). While overall IBA1 expression did not increase significantly (Fig.8E), there was an increase in the density of IBA1-positive cells (p=0.0135, student's t-test, n=6/genotype, Fig. 8F) in the BLA of Thy1-aSyn mice. The observation of increased density likely correlates with the apparent increased size of the cell body of the activated microglia. Thus, α-syn pathology coincides with neuroinflammation in this brain region.

Alpha-synuclein pathology and neuroinflammatory processes may result in specific neurotoxicity in the BLA. Considering the role which GABAergic interneurons and their micro-circuitry play in anxiety and fear learning (Babaev et al., 2018; Duvarci and Pare, 2014; Ehrlich et al., 2009; Krabbe et al., 2018; Wolff et al., 2014; Yau et al., 2020) together with the presence of α-syn aggregates in parvalbumin neurons in the amygdala of PD patients (Flores-Cuadrado et al., 2017), we hypothesized that loss of these neurons could represent a mechanism for increased fear response in Thy1-aSyn mice. We observed a reduced density of parvalbumin-positive neurons in the BLA in Thy1-aSyn mice compared to wild-type (p=0.0256, student's t-test, n=6/genotype Fig. 9E), while no changes were observed in the overall protein expression of parvalbumin and calbindin (not shown), and in the density of calbindin-positive neurons (Fig. 9F). Loss of inhibitory interneurons may modulate neuronal activity in this region, therefore we quantified c-Fos expression as immediate early marker for neuronal activity (Fig. 10). The number of c-Fos positive cells was reduced in naive Thy1-aSyn mice (p=0.013, student's t-test, Fig. 10A, B). While a

large fraction of these neurons are positive for parvalbumin, quantification of double-labeled neurons indicate that other cell types are also involved in the observed c-Fos reduction (Fig. 10C, D).

DISCUSSION

In this study, we examined whether wild-type human α-syn overexpression alters fear processing in Thy1-aSyn mice, and if these changes were accompanied by α-syn-associated neuropathology. We subjected mice to Pavlovian fear conditioning procedures as they directly measure fear learning and memory and potentially limit the impact of differences in general activity and motor function (Crawley, 2008; Eltokhi et al., 2020). We observed that an increased fear phenotype is present at an early age in Thy1-aSyn mice, prior to dopamine loss (Lam et al. 2011), and thereby coincides with a broad range of non-motor and motor dysfunction relevant to PD in this model (Chesselet et al., 2012; Chesselet and Richter, 2011; McDowell and Chesselet, 2012; McDowell et al., 2014). Furthermore, behavioral changes were accompanied by the presence of α-syn accumulation and aggregation, microgliosis and a loss of parvalbumin positive neurons in the BLA, a brain region that plays a major role in the regulation of fear responses.

Increased tone fear as an early phenotype in α-syn overexpressing mice

The importance of non-motor symptoms in PD is being increasingly recognized, prompting the need to develop animal models of these deficits to complement the study of the more classical motor deficits and to include these endpoints into pre-clinical trials of potential neuroprotective strategies (Chesselet, 2008; Pfeiffer, 2016). Increasing evidence implicates α-syn in both sporadic and familial forms of PD (Braak et al., 2002; Edwards et al., 2010; Klein and Westenberger, 2012). Therefore, α-syn overexpressing mice are widely used to model PD (Chesselet and Richter, 2011). Several studies show mice harboring the rare A53T mutated form of α-syn develop reduced anxiety-like behavior (Paumier et al., 2013; Rothman et al., 2013; Yamakado et al., 2012) or decreased freezing in Pavlovian fear conditioning during old age (Freichel et al., 2007). Decreased freezing during the first minute of exposure to contextual fear conditioning was also observed in mice intrastriatally injected with α-syn fibrils (Stoyka et al., 2020). In PD, however, patients show increased anxiety, which occurs early in the disease and is difficult to manage with available therapeutic options (Duncan et al., 2014; Postuma et al., 2012). Here we used mice overexpressing human wild-type α-syn under the pan-neuronal Thy-1 promoter that have been previously characterized extensively for the progression of dopamine pathology, motor anomalies, and a variety of non-motor deficits (Chesselet et al., 2012; Chesselet and Richter, 2011; McDowell and Chesselet, 2012; McDowell et al., 2014; Rockenstein et al., 2002). We used young mice with the goal to replicate early psychiatric aspects of PD which can serve as endpoints to test disease-modifying interventions. We show that these mice display enhanced fear responses in Pavlovian fear conditioning, consistent with an overall increased fear phenotype.

We took advantage of research on Pavlovian fear conditioning and its various components that has identified specific neuronal structures and systems within the fear circuitry (Kochli

et al., 2015; Maren, 2008). These insights are helpful to direct pathological studies to specific brain regions and neuronal circuitries, depending on the observed behavioral phenotype. One particularly interesting element of our findings is that Thy1-aSyn mice showed significant enhancements in tone but not context fear. This suggests that increased levels of α-syn may operate in a more selective manner at specific brain sites within the fear circuitry. The overall enhancement in tone fear may point to dysfunction in the amygdala (Fanselow and LeDoux, 1999; Jimenez and Maren, 2009). Our additional findings that Thy1-aSyn mice are deficient in retaining extinction memories further supports the idea that amygdala circuitry may be functioning in a maladaptive manner in PD and could have implications for the long-term effects of anxiolytic therapy in PD.

Alpha-syn aggregation, neuroinflammation, and loss of parvalbumin neurons in the BLA as pathological correlates for increased fear responding.

Increased expression of α-syn and Ser129P-α-syn and formation of insoluble aggregates in the BLA of Thy1-aSyn mice further support the hypothesis that the impaired function of the amygdala may play a central role in the enhanced anxiety seen in PD. Alpha-synuclein is selectively and extensively phosphorylated at serine 129 in PD and other synucleinopathies, and reducing α-syn phosphorylation is beneficial in Thy1-aSyn mice (Lee et al., 2011). Proteinase K-resistant insoluble α-syn is present in brains of patients with different Lewy body diseases (Neumann et al., 2004). Interestingly, α-syn knock-out mice do not show changes in anxiety-like behaviors (Peña-Oliver et al., 2010), supporting the notion that a gain of toxic function downstream of α-syn accumulation likely accounts for the fear phenotype observed in Thy1-aSyn mice (Chesselet et al., 2012).

Neuroinflammation is an important contributor to PD pathogenesis (Hirsch et al., 2012; Troncoso-Escudero et al., 2018) and could result from α-syn toxicity in PD. Although neuroinflammation may not be the primary cause of PD, numerous studies indicate that chronic inflammation occurs in affected brain regions and is crucial for disease progression (McGeer and McGeer, 2004). Interestingly, both wild-type and mutant α-syn, can promote pro-inflammatory cascades in microglia (Allen Reish and Standaert, 2015; Hoenen et al., 2016), and in Thy1-aSyn mice microgliosis is associated with α-syn pathology in the striatum and substantia nigra (Watson et al., 2012). Therefore, observation that accumulation of phosphorylated α-syn and the presence of proteinase K-resistant aggregates in the amygdala are accompanied by microglial activation is in line with previous observations.

Parvalbumin interneurons and microcircuits in the amygdala play a significant role in mood and emotional responses including anxiety and fear (Duvarci and Pare, 2014; Krabbe et al., 2018; Yau et al., 2020). Interestingly, parvalbumin neurons in amygdala are specifically affected by α-syn-associated pathology in PD: α-syn aggregations have been detected in the parvalbumin neurons in amygdala of PD patients (Flores-Cuadrado et al., 2017). The loss of inhibitory, GABA-producing parvalbumin interneurons could explain, at least partially, the observed phenotype in Thy1-aSyn mice. Indeed, data suggest that inhibitory amygdala circuits regulate associative fear conditioning (Krabbe et al., 2018). Further, a study from Wolff et al. (Wolff et al., 2014) directly demonstrated that the strength of aversive memories is under the bi-directional control of amygdala parvalbumin interneuron activity

and that parvalbumin neurons control fear learning through disinhibition. Since parvalbumin immunopositive neurons make up about 40% of GABAergic interneurons (Capogna, 2014; Prager et al., 2016) it is possible that the observed loss significantly impacts GABA levels in amygdala as well. Different studies observed that impairment of GABA production and transmission promotes anxiety and disrupts the regulation of fear responses (Heldt et al., 2012; Jie et al., 2018). A loss of parvalbumin neurons in other brain regions was observed in chemically induced and transgenic animal models of PD (Fernández-Suárez et al., 2012; Stanojlovic et al., 2019b), and may further contribute to PD pathophysiology. Contrary to our results and findings in patients, in mice injected intrastriatally with α-syn fibrils, inclusions specifically localized to excitatory neurons in the amygdala. Interestingly, cell loss of the total number of neurons in the amygdala was 18% (p = 0.055) in this model, which may indicate loss of specific neuronal subpopulations (Stoyka et al., 2020). The observed excitatory neuron-associated α-syn pathology might be because those neurons send their projections to the dorsolateral striatum, the region where the pre-formed fibrils were injected (Stoyka et al., 2020). Parvalbumin neurons are interneurons that form local circuits in the BLA (Woodruff and Sah, 2007). In Thy1-aSyn mice NeuN positive cells of the BLA accumulate p-α-syn (Fig. 6), which together with the observed microgliosis can initiate neurodegeneration (Kwon and Koh, 2020). The loss of inhibitory neurons promotes overt excitation and thus excitotoxicity (Dong et al., 2009), which parvalbumin neurons are particularly vulnerable to (Moga et al., 2002; Van Den Bosch et al., 2002). Of note, a lack of appropriate maturation can result in reduced parvalbumin expression in interneurons (Bode et al., 2017). Neurogenic precursor cells that develop into interneurons were described in the BLA of adult mice (Jhaveri et al., 2018). As adult neurogenesis is impaired in the hippocampus of Thy1-aSyn mice (Bender et al., 2021), it is conceivable that this process may also be altered in the BLA, requiring further investigation.

The examination of c-Fos immediate early gene protein expression, which is used as a marker of neuronal activation (Kawashima et al., 2014), revealed reduced number of neurons expressing c-Fos in Thy1-aSyn mice compared to WT littermates without prior fear conditioning. These c-Fos expressing neurons were in part also parvalbumin-positive, but the overall number of c-Fos positive neurons was low as expected without specific stimulation. For example, fear acquisition and acute and chronic stress are associated with increased c-Fos expression in the BLA (Hofmann, 2008; Kovács et al., 2018), which could further shift the state of neuronal excitation in transgenic mice. Further investigation is required to draw solid conclusion on the impact of α-syn pathology on BLA neuronal activity upon fear conditioning. Of note, although we observed a trend towards reduction (p=0.077), calbindin positive cell numbers were not significantly reduced, which suggests that parvalbumin positive neurons are more susceptible to α-syn-associated pathology in this region. These novel insights provide the basis for further studying how alterations of the complex inhibitory networks in the amygdala, which comprises a multitude of neuronal and synaptic subtypes with highly diverse functions (Babaev et al., 2018; Lee et al., 2013), contributes to early fear and anxiety in PD. Furthermore, cortical regions also show overexpression of α-syn in Thy1-aSyn mice (Chesselet et al., 2012), and while the amygdala clearly has a critical role in cued fear conditioning, α-syn induced abnormalities in the cortical-amygdala circuitry may also be playing a role.

Conclusion

In this study, we detected and described increases in fear responding in the Thy1-aSyn transgenic mouse model, replicating the increased anxiety observed in PD patients. Aside from accumulation of proteinase K-resistant aggregates and phosphorylated α-syn, we observed microgliosis and loss of parvalbumin positive neurons in the BLA of Thy1-aSyn mice as probable mechanistic culprits. Better understanding of these mechanisms in PD will help the development of novel treatments including the application of available anxiolytic compounds for treating mood disorders and emotional disturbances in PD.

Acknowledgements

Data availability

Data supporting the figures of this manuscript are available from the corresponding author upon reasonable request.

Abbreviations

PD	Parkinson's Disease
α-syn	α-synuclein
Calbindin	Calbindin D28K
GABA	γ-aminobutyric acid
BLA	Basolateral nucleus of the amygdala
PCR	Polymerase chain reaction
BL	Baseline
ITI	inter-trial interval
SIH	Stress-induced hyperthermia
PMT	Photomultiplier tube
NIR	Automated near infrared

References

Allen Reish HE, Standaert DG, 2015. Role of α-synuclein in inducing innate and adaptive immunity in Parkinson disease. J. Park. Dis5, 1–19. 10.3233/JPD-140491

Babaev O, Piletti Chatain C, Krueger-Burg D., 2018. Inhibition in the amygdala anxiety circuitry. Exp. Mol. Med50, 1–16. 10.1038/s12276-018-0063-8

Bender H, Fietz SA, Richter F, Stanojlovic M., 2021. Alpha-Synuclein Pathology Coincides With Increased Number of Early Stage Neural Progenitors in the Adult Hippocampus. Front. Cell Dev. Biol0. 10.3389/fcell.2021.691560

Bertrand E, Lechowicz W, Szpak GM, Lewandowska E, Dymecki J, Wierzba-Bobrowicz T., 2004. Limbic neuropathology in idiopathic Parkinson's disease with concomitant dementia. Folia Neuropathol. 42, 141–150. [PubMed: 15535032]

Bode C, Richter F, Spröte C, Brigadski T, Bauer A, Fietz S, Fritschy J-M, Richter A., 2017. Altered postnatal maturation of striatal GABAergic interneurons in a phenotypic animal model of dystonia. Exp. Neurol287, 44–53. 10.1016/j.expneurol.2016.10.013 [PubMed: 27780732]

Braak H, Del Tredici K, Bratzke H, Hamm-Clement J, Sandmann-Keil D, Rüb U., 2002. Staging of the intracerebral inclusion body pathology associated with idiopathic Parkinson's disease (preclinical and clinical stages). J. Neurol249Suppl 3, III/1–5. 10.1007/s00415-002-1301-4

Braak H, Del Tredici K, Rüb U, de Vos RAI, Jansen Steur ENH, Braak E., 2003. Staging of brain pathology related to sporadic Parkinson's disease. Neurobiol. Aging24, 197–211. 10.1016/s0197-4580(02)00065-9 [PubMed: 12498954]

Caillard O, Moreno H, Schwaller B, Llano I, Celio MR, Marty A., 2000. Role of the calcium-binding protein parvalbumin in short-term synaptic plasticity. Proc. Natl. Acad. Sci97, 13372–13377. 10.1073/pnas.230362997 [PubMed: 11069288]

Capogna M., 2014. GABAergic cell type diversity in the basolateral amygdala. Curr. Opin. Neurobiol26, 110–116. 10.1016/j.conb.2014.01.006 [PubMed: 24486420]

Chen JJ, Marsh L., 2014. Anxiety in Parkinson's disease: identification and management. Ther. Adv. Neurol. Disord7, 52–59. 10.1177/1756285613495723 [PubMed: 24409202]

Chesselet M-F, 2008. In vivo alpha-synuclein overexpression in rodents: a useful model of Parkinson's disease?Exp. Neurol209, 22–27. 10.1016/j.expneurol.2007.08.006 [PubMed: 17949715]

Chesselet M-F, Richter F., 2011. Modelling of Parkinson's disease in mice. Lancet Neurol. 10, 1108–1118. 10.1016/S1474-4422(11)70227-7 [PubMed: 22094131]

Chesselet M-F, Richter F, Zhu C, Magen I, Watson MB, Subramaniam SR, 2012. A Progressive Mouse Model of Parkinson's Disease: The Thy1-aSyn ("Line 61") Mice. Neurotherapeutics9, 297–314. 10.1007/s13311-012-0104-2 [PubMed: 22350713]

Connolly B, Fox SH, 2014. Treatment of cognitive, psychiatric, and affective disorders associated with Parkinson's disease. Neurother. J. Am. Soc. Exp. Neurother11, 78–91. 10.1007/s13311-013-0238-x

Crawley JN, 2008. Behavioral Phenotyping Strategies for Mutant Mice. Neuron57, 809–818. 10.1016/j.neuron.2008.03.001 [PubMed: 18367082]

Cushman JD, Moore MD, Jacobs NS, Olsen RW, Fanselow MS, 2011. Behavioral pharmacogenetic analysis on the role of the α4 GABAA receptor subunit in the ethanol-mediated impairment of hippocampus-dependent contextual learning. Alcohol. Clin. Exp. Res35, 1948–1959. 10.1111/j.1530-0277.2011.01546.x [PubMed: 21943327]

De Oca BM, DeCola JP, Maren S, Fanselow MS, 1998. Distinct Regions of the Periaqueductal Gray Are Involved in the Acquisition and Expression of Defensive Responses. J. Neurosci18, 3426–3432. 10.1523/JNEUROSCI.18-09-03426.1998 [PubMed: 9547249]

Dickson DW, Fujishiro H, Orr C, DelleDonne A, Josephs KA, Frigerio R, Burnett M, Parisi JE, Klos KJ, Ahlskog JE, 2009. Neuropathology of non-motor features of Parkinson disease. Parkinsonism Relat. Disord15Suppl 3, S1–5. 10.1016/S1353-8020(09)70769-2

Dong X, Wang Y, Qin Z., 2009. Molecular mechanisms of excitotoxicity and their relevance to pathogenesis of neurodegenerative diseases. Acta Pharmacol. Sin30, 379–387. 10.1038/aps.2009.24 [PubMed: 19343058]

Duncan GW, Khoo TK, Yarnall AJ, O'Brien JT, Coleman SY, Brooks DJ, Barker RA, Burn DJ, 2014. Health-related quality of life in early Parkinson's disease: the impact of nonmotor symptoms. Mov. Disord. Off. J. Mov. Disord. Soc29, 195–202. 10.1002/mds.25664

Duvarci S, Pare D., 2014. Amygdala Microcircuits Controlling Learned Fear. Neuron82, 966–980. 10.1016/j.neuron.2014.04.042 [PubMed: 24908482]

Edwards TL, Scott WK, Almonte C, Burt A, Powell EH, Beecham GW, Wang L, Züchner S, Konidari I, Wang G, Singer C, Nahab F, Scott B, Stajich JM, Pericak-Vance M, Haines J, Vance JM, Martin ER, 2010. Genome-wide association study confirms SNPs in SNCA and the MAPT region as common risk factors for Parkinson disease. Ann. Hum. Genet74, 97–109. 10.1111/j.1469-1809.2009.00560.x [PubMed: 20070850]

Ehrlich I, Humeau Y, Grenier F, Ciocchi S, Herry C, Lüthi A., 2009. Amygdala inhibitory circuits and the control of fear memory. Neuron62, 757–771. 10.1016/j.neuron.2009.05.026 [PubMed: 19555645]

Eltokhi A, Kurpiers B, Pitzer C., 2020. Behavioral tests assessing neuropsychiatric phenotypes in adolescent mice reveal strain- and sex-specific effects. Sci. Rep10, 11263. 10.1038/s41598-020-67758-0 [PubMed: 32647155]

Fanselow MS, 1982. The postshock activity burst. Anim. Learn. Behav10, 448–454. 10.3758/BF03212284

Fanselow MS, LeDoux JE, 1999. Why we think plasticity underlying Pavlovian fear conditioning occurs in the basolateral amygdala. Neuron23, 229–232. 10.1016/s0896-6273(00)80775-8 [PubMed: 10399930]

Fernagut PO, Hutson CB, Fleming SM, Tetreaut NA, Salcedo J, Masliah E, Chesselet MF, 2007. Behavioral and histopathological consequences of paraquat intoxication in mice: effects of alpha-synuclein over-expression. Synap. N. Y. N61, 991–1001. 10.1002/syn.20456

Fernández-Suárez D, Celorrio M, Lanciego JL, Franco R, Aymerich MS, 2012. Loss of parvalbumin-positive neurons from the globus pallidus in animal models of Parkinson disease. J. Neuropathol. Exp. Neurol71, 973–982. 10.1097/NEN.0b013e3182717cba [PubMed: 23044920]

Fleming SM, Tetreault NA, Mulligan CK, Hutson CB, Masliah E, Chesselet M-F, 2008. Olfactory deficits in mice overexpressing human wildtype alpha-synuclein. Eur. J. Neurosci28, 247–256. 10.1111/j.1460-9568.2008.06346.x [PubMed: 18702696]

Flores-Cuadrado A, Ubeda-Bañon I, Saiz-Sanchez D, Martinez-Marcos A., 2017. α-Synucleinopathy in the Human Amygdala in Parkinson Disease: Differential Vulnerability of Somatostatin- and Parvalbumin-Expressing Neurons. J. Neuropathol. Exp. Neurol76, 754–758. 10.1093/jnen/nlx054 [PubMed: 28859333]

Foehring RC, Zhang XF, Lee J c. f., Callaway, J.C., 2009. Endogenous Calcium Buffering Capacity of Substantia Nigral Dopamine Neurons. J. Neurophysiol 102, 2326–2333. 10.1152/jn.00038.2009 [PubMed: 19675297]

Freichel C, Neumann M, Ballard T, Müller V, Woolley M, Ozmen L, Borroni E, Kretzschmar HA, Haass C, Spooren W, Kahle PJ, 2007. Age-dependent cognitive decline and amygdala pathology in alpha-synuclein transgenic mice. Neurobiol. Aging28, 1421–1435. 10.1016/j.neurobiolaging.2006.06.013 [PubMed: 16872721]

GBD 2015 Neurological Disorders Collaborator Group, 2017. Global, regional, and national burden of neurological disorders during 1990–2015: a systematic analysis for the Global Burden of Disease Study 2015. Lancet Neurol. 16, 877–897. 10.1016/S1474-4422(17)30299-5 [PubMed: 28931491]

George S, Buuse M, Mok SS, Masters C, Culvenor J., 2008. α-Synuclein transgenic mice exhibit reduced anxiety-like behaviour. Exp. Neurol10.1016/j.expneurol.2007.12.017

Gerstenberger J, Bauer A, Helmschrodt C, Richter A, Richter F., 2016. The novel adaptive rotating beam test unmasks sensorimotor impairments in a transgenic mouse model of Parkinson's disease. Behav. Brain Res304, 102–110. 10.1016/j.bbr.2016.02.017 [PubMed: 26880341]

Heldt SA, Mou L, Ressler KJ, 2012. In vivo knockdown of GAD67 in the amygdala disrupts fear extinction and the anxiolytic-like effect of diazepam in mice. Transl. Psychiatry2, e181–e181. 10.1038/tp.2012.101 [PubMed: 23149445]

Hirsch EC, Vyas S, Hunot S., 2012. Neuroinflammation in Parkinson's disease. Parkinsonism Relat. Disord18Suppl 1, S210–212. 10.1016/S1353-8020(11)70065-7 [PubMed: 22166438]

Hoenen C, Gustin A, Birck C, Kirchmeyer M, Beaume N, Felten P, Grandbarbe L, Heuschling P, Heurtaux T., 2016. Alpha-Synuclein Proteins Promote Pro-Inflammatory Cascades in Microglia: Stronger Effects of the A53T Mutant. PLOS ONE11, e0162717. 10.1371/journal.pone.0162717 [PubMed: 27622765]

Hofmann SG, 2008. Cognitive processes during fear acquisition and extinction in animals and humans. Clin. Psychol. Rev28, 199–210. 10.1016/j.cpr.2007.04.009 [PubMed: 17532105]

Jhaveri DJ, Tedoldi A, Hunt S, Sullivan R, Watts NR, Power JM, Bartlett PF, Sah P., 2018. Evidence for newly generated interneurons in the basolateral amygdala of adult mice. Mol. Psychiatry23, 521–532. 10.1038/mp.2017.134 [PubMed: 28809399]

Jie F, Yin G, Yang W, Yang M, Gao S, Lv J, Li B., 2018. Stress in Regulation of GABA Amygdala System and Relevance to Neuropsychiatric Diseases. Front. Neurosci12. 10.3389/fnins.2018.00562

Jimenez SA, Maren S., 2009. Nuclear disconnection within the amygdala reveals a direct pathway to fear. Learn. Mem16, 766–768. 10.1101/lm.1607109 [PubMed: 19933881]

Kawashima T, Okuno H, Bito H., 2014. A new era for functional labeling of neurons: activity-dependent promoters have come of age. Front. Neural Circuits8. 10.3389/fncir.2014.00037

Klein C, Westenberger A., 2012. Genetics of Parkinson's Disease. Cold Spring Harb. Perspect. Med2. 10.1101/cshperspect.a008888

Kochli DE, Thompson EC, Fricke EA, Postle AF, Quinn JJ, 2015. The amygdala is critical for trace, delay, and contextual fear conditioning. Learn. Mem22, 92–100. 10.1101/lm.034918.114 [PubMed: 25593295]

Kovács LÁ, Schiessl JA, Nafz AE, Csernus V, Gaszner B., 2018. Both Basal and Acute Restraint Stress-Induced c-Fos Expression Is Influenced by Age in the Extended Amygdala and Brainstem Stress Centers in Male Rats. Front. Aging Neurosci10. 10.3389/fnagi.2018.00248

Krabbe S, Gründemann J, Lüthi A., 2018. Amygdala Inhibitory Circuits Regulate Associative Fear Conditioning. Biol. Psychiatry83, 800–809. 10.1016/j.biopsych.2017.10.006 [PubMed: 29174478]

Kwon HS, Koh S-H, 2020. Neuroinflammation in neurodegenerative disorders: the roles of microglia and astrocytes. Transl. Neurodegener9, 42. 10.1186/s40035-020-00221-2 [PubMed: 33239064]

Lam HA, Wu N, Cely I, Kelly RL, Hean S, Richter F, Magen I, Cepeda C, Ackerson LC, Walwyn W, Masliah E, Chesselet M-F, Levine MS, Maidment NT, 2011. Elevated tonic extracellular dopamine concentration and altered dopamine modulation of synaptic activity precede dopamine loss in the striatum of mice overexpressing human α-synuclein. J. Neurosci. Res89, 1091–1102. 10.1002/jnr.22611 [PubMed: 21488084]

Lee K-W, Chen W, Junn E, Im J-Y, Grosso H, Sonsalla PK, Feng X, Ray N, Fernandez JR, Chao Y, Masliah E, Voronkov M, Braithwaite SP, Stock JB, Mouradian MM, 2011. Enhanced phosphatase activity attenuates α-synucleinopathy in a mouse model. J. Neurosci. Off. J. Soc. Neurosci31, 6963–6971. 10.1523/JNEUROSCI.6513-10.2011

Lee S, Kim S-J, Kwon O-B, Lee JH, Kim J-H, 2013. Inhibitory networks of the amygdala for emotional memory. Front. Neural Circuits7. 10.3389/fncir.2013.00129

Lu X-H, Fleming SM, Meurers B, Ackerson LC, Mortazavi F, Lo V, Hernandez D, Sulzer D, Jackson GR, Maidment NT, Chesselet M-F, Yang XW, 2009. Bacterial Artificial Chromosome Transgenic Mice Expressing a Truncated Mutant Parkin Exhibit Age-Dependent Hypokinetic Motor Deficits, Dopaminergic Neuron Degeneration, and Accumulation of Proteinase K-Resistant α-Synuclein. J. Neurosci29, 1962–1976. 10.1523/JNEUROSCI.5351-08.2009 [PubMed: 19228951]

Maren S., 2008. Pavlovian fear conditioning as a behavioral assay for hippocampus and amygdala function: cautions and caveats. Eur. J. Neurosci28, 1661–1666. 10.1111/j.1460-9568.2008.06485.x [PubMed: 18973583]

McDowell K, Chesselet M-F, 2012. Animal models of the non-motor features of Parkinson's disease. Neurobiol. Dis46, 597–606. 10.1016/j.nbd.2011.12.040 [PubMed: 22236386]

McDowell KA, Shin D, Roos KP, Chesselet M-F, 2014. Sleep dysfunction and EEG alterations in mice overexpressing alpha-synuclein. J. Park. Dis4, 531–539. 10.3233/JPD-140374

McGeer PL, McGeer EG, 2004. Inflammation and neurodegeneration in Parkinson's disease. Parkinsonism Relat. Disord10Suppl 1, S3–7. 10.1016/j.parkreldis.2004.01.005 [PubMed: 15109580]

Moga D, Hof PR, Vissavajjhala P, Moran TM, Morrison JH, 2002. Parvalbumin-containing interneurons in rat hippocampus have an AMPA receptor profile suggestive of vulnerability to excitotoxicity. J. Chem. Neuroanat23, 249–253. 10.1016/s0891-0618(02)00012-1 [PubMed: 12048108]

Morris M, Sanchez PE, Verret L, Beagle AJ, Guo W, Dubal D, Ranasinghe KG, Koyama A, Ho K, Yu G, Vossel KA, Mucke L., 2015. Network dysfunction in α-synuclein transgenic mice and human Lewy body dementia. Ann. Clin. Transl. Neurol2, 1012–1028. 10.1002/acn3.257 [PubMed: 26732627]

Mufti S, LaFaver K., 2020. Mood Disorders in Parkinson's Disease. Psychiatr. Ann50, 95–99. 10.3928/00485713-20200203-01

Neumann M, Müller V, Kretzschmar HA, Haass C, Kahle PJ, 2004. Regional distribution of proteinase K-resistant alpha-synuclein correlates with Lewy body disease stage. J. Neuropathol. Exp. Neurol63, 1225–1235. 10.1093/jnen/63.12.1225 [PubMed: 15624759]

Olivier B, Zethof T, Pattij T, van Boogaert M, van Oorschot R, Leahy C, Oosting R, Bouwknecht A, Veening J, van der Gugten J, Groenink L., 2003. Stress-induced hyperthermia and anxiety: pharmacological validation. Eur. J. Pharmacol463, 117–132. 10.1016/s0014-2999(03)01326-8 [PubMed: 12600705]

Paumier KL, Rizzo SJS, Berger Z, Chen Y, Gonzales C, Kaftan E, Li L, Lotarski S, Monaghan M, Shen W, Stolyar P, Vasilyev D, Zaleska M, Hirst WD, Dunlop J., 2013. Behavioral Characterization of A53T Mice Reveals Early and Late Stage Deficits Related to Parkinson's Disease. PLOS ONE8, e70274. 10.1371/journal.pone.0070274 [PubMed: 23936403]

Paxinos G, Franklin KBJ, 2004. The mouse brain in stereotaxic coordinates, 2nd ed.,Compact ed. ed. Academic, London.

Peña-Oliver Y, Buchman VL, Stephens DN, 2010. Lack of involvement of alpha-synuclein in unconditioned anxiety in mice. Behav. Brain Res209, 234–240. 10.1016/j.bbr.2010.01.049 [PubMed: 20138921]

Pfeiffer RF, 2016. Non-motor symptoms in Parkinson's disease. Parkinsonism Relat. Disord22Suppl 1, S119–122. 10.1016/j.parkreldis.2015.09.004 [PubMed: 26372623]

Poewe W, Seppi K, Tanner CM, Halliday GM, Brundin P, Volkmann J, Schrag A-E, Lang AE, 2017. Parkinson disease. Nat. Rev. Dis. Primer3, 1–21. 10.1038/nrdp.2017.13

Postuma RB, Aarsland D, Barone P, Burn DJ, Hawkes CH, Oertel W, Ziemssen T., 2012. Identifying prodromal Parkinson's disease: pre-motor disorders in Parkinson's disease. Mov. Disord. Off. J. Mov. Disord. Soc27, 617–626. 10.1002/mds.24996

Prager EM, Bergstrom HC, Wynn GH, Braga MFM, 2016. The Basolateral Amygdala GABAergic System in Health and Disease. J. Neurosci. Res94, 548–567. 10.1002/jnr.23690 [PubMed: 26586374]

Rahman MM, Uddin MJ, Chowdhury JH, Chowdhury TI, 2014. Effect of levodopa and carbidopa on non-motor symptoms and signs of Parkinson's disease. Mymensingh Med. J. MMJ23, 18–23. [PubMed: 24584367]

Ressler KJ, 2010. Amygdala Activity, Fear, and Anxiety: Modulation by Stress. Biol. Psychiatry67, 1117–1119. 10.1016/j.biopsych.2010.04.027 [PubMed: 20525501]

Rocca WA, 2018. The burden of Parkinson's disease: a worldwide perspective. Lancet Neurol. 17, 928–929. 10.1016/S1474-4422(18)30355-7 [PubMed: 30287052]

Rockenstein E, Mallory M, Hashimoto M, Song D, Shults CW, Lang I, Masliah E., 2002. Differential neuropathological alterations in transgenic mice expressing alpha-synuclein from the platelet-derived growth factor and Thy-1 promoters. J. Neurosci. Res68, 568–578. 10.1002/jnr.10231 [PubMed: 12111846]

Rothman SM, Griffioen KJ, Vranis N, Ladenheim B, Cong W, Cadet J-L, Haran J, Martin B, Mattson MP, 2013. Neuronal expression of familial Parkinson's disease A53T α-synuclein causes early motor impairment, reduced anxiety and potential sleep disturbances in mice. J. Park. Dis3, 215–229. 10.3233/JPD-120130

Schrag A, Taddei RN, 2017. Chapter Twenty - Depression and Anxiety in Parkinson's Disease, in: Chaudhuri KR, Titova N (Eds.), International Review of Neurobiology, Nonmotor Parkinson's: The Hidden Face. Academic Press, pp. 623–655. 10.1016/bs.irn.2017.05.024

Sorrentino ZA, Goodwin MS, Riffe CJ, Dhillon J-KS, Xia Y, Gorion K-M, Vijayaraghavan N, McFarland KN, Golbe LI, Yachnis AT, Giasson BI, 2019. Unique α-synuclein pathology within the amygdala in Lewy body dementia: implications for disease initiation and progression. Acta Neuropathol. Commun7, 142. 10.1186/s40478-019-0787-2 [PubMed: 31477175]

Spillantini MG, Schmidt ML, Lee VM, Trojanowski JQ, Jakes R, Goedert M., 1997. Alpha-synuclein in Lewy bodies. Nature388, 839–840. 10.1038/42166 [PubMed: 9278044]

Stanojlovic M, Pallais JP, Kotz CM, 2019a. Chemogenetic Modulation of Orexin Neurons Reverses Changes in Anxiety and Locomotor Activity in the A53T Mouse Model of Parkinson's Disease. Front. Neurosci13. 10.3389/fnins.2019.00702

Stanojlovic M, Pallais Yllescas JP, Vijayakumar A, Kotz C., 2019b. Early Sociability and Social Memory Impairment in the A53T Mouse Model of Parkinson's Disease Are Ameliorated by Chemogenetic Modulation of Orexin Neuron Activity. Mol. Neurobiol56, 8435–8450. 10.1007/s12035-019-01682-x [PubMed: 31250383]

Steimer T., 2002. The biology of fear- and anxiety-related behaviors. Dialogues Clin. Neurosci4, 231–249. [PubMed: 22033741]

Stoyka LE, Arrant AE, Thrasher DR, Russell DL, Freire J, Mahoney CL, Narayanan A, Dib AG, Standaert DG, Volpicelli-Daley LA, 2020. Behavioral defects associated with amygdala and cortical dysfunction in mice with seeded α-synuclein inclusions. Neurobiol. Dis134, 104708. 10.1016/j.nbd.2019.104708 [PubMed: 31837424]

Surmeier DJ, Schumacker PT, Guzman JD, Ilijic E, Yang B, Zampese E., 2017. Calcium and Parkinson's disease. Biochem. Biophys. Res. Commun483, 1013–1019. 10.1016/j.bbrc.2016.08.168 [PubMed: 27590583]

Troncoso-Escudero P, Parra A, Nassif M, Vidal RL, 2018. Outside in: Unraveling the Role of Neuroinflammation in the Progression of Parkinson's Disease. Front. Neurol9. 10.3389/fneur.2018.00860

Tysnes O-B, Storstein A., 2017. Epidemiology of Parkinson's disease. J. Neural Transm. Vienna Austria 1996124, 901–905. 10.1007/s00702-017-1686-y

Van Den Bosch L, Schwaller B, Vleminckx V, Meijers B, Stork S, Ruehlicke T, Van Houtte E, Klaassen H, Celio MR, Missiaen L, Robberecht W, Berchtold MW, 2002. Protective effect of parvalbumin on excitotoxic motor neuron death. Exp. Neurol174, 150–161. 10.1006/exnr.2001.7858 [PubMed: 11922657]

van der Putten H, Wiederhold KH, Probst A, Barbieri S, Mistl C, Danner S, Kauffmann S, Hofele K, Spooren WP, Ruegg MA, Lin S, Caroni P, Sommer B, Tolnay M, Bilbe G., 2000. Neuropathology in mice expressing human alpha-synuclein. J. Neurosci. Off. J. Soc. Neurosci20, 6021–6029.

Villalobos CA, Wu Q, Lee PH, May PJ, Basso MA, 2018. Parvalbumin and GABA Microcircuits in the Mouse Superior Colliculus. Front. Neural Circuits12. 10.3389/fncir.2018.00035

Wang L, Magen I, Yuan P-Q, Subramaniam SR, Richter F, Chesselet M-F, Taché Y., 2012. Mice overexpressing wild-type human alpha-synuclein display alterations in colonic myenteric ganglia and defecation. Neurogastroenterol. Motil. Off. J. Eur. Gastrointest. Motil. Soc24, e425–436. 10.1111/j.1365-2982.2012.01974.x

Watson MB, Richter F, Lee SK, Gabby L, Wu J, Masliah E, Effros RB, Chesselet M-F, 2012. Regionally-specific microglial activation in young mice over-expressing human wildtype alpha-synuclein. Exp. Neurol237, 318–334. 10.1016/j.expneurol.2012.06.025 [PubMed: 22750327]

Wolff SBE, Gründemann J, Tovote P, Krabbe S, Jacobson GA, Müller C, Herry C, Ehrlich I, Friedrich RW, Letzkus JJ, Lüthi A., 2014. Amygdala interneuron subtypes control fear learning through disinhibition. Nature509, 453–458. 10.1038/nature13258 [PubMed: 24814341]

Woodruff AR, Sah P., 2007. Networks of Parvalbumin-Positive Interneurons in the Basolateral Amygdala. J. Neurosci27, 553–563. 10.1523/JNEUROSCI.3686-06.2007 [PubMed: 17234587]

Yamakado H, Moriwaki Y, Yamasaki N, Miyakawa T, Kurisu J, Uemura K, Inoue H, Takahashi M, Takahashi R., 2012. α-Synuclein BAC transgenic mice as a model for Parkinson's disease manifested decreased anxiety-like behavior and hyperlocomotion. Neurosci. Res73, 173–177. 10.1016/j.neures.2012.03.010 [PubMed: 22475625]

Yamanishi T, Tachibana H, Oguru M, Matsui K, Toda K, Okuda B, Oka N., 2013. Anxiety and depression in patients with Parkinson's disease. Intern. Med. Tokyo Jpn52, 539–545. 10.2169/internalmedicine.52.8617

Yau JO-Y, Chaichim C, Power JM, McNally GP, 2020. Basolateral amygdala parvalbumin neurons report aversive prediction error to constrain fear learning. bioRxiv2020.09.22.307561. 10.1101/2020.09.22.307561

Zaichick SV, McGrath KM, Caraveo G., 2017. The role of Ca2+ signaling in Parkinson's disease. Dis. Model. Mech10, 519–535. 10.1242/dmm.028738 [PubMed: 28468938]

Zou D, Chen L, Deng D, Jiang D, Dong F, McSweeney C, Zhou Y, Liu L, Chen G, Wu Y, Mao Y., 2016. DREADD in parvalbumin interneurons of the dentate gyrus modulates anxiety, social interaction and memory extinction. Curr. Mol. Med16, 91–102. 10.2174/1566524016666151222150024 [PubMed: 26733123]

Highlights

- Mice overexpressing alpha-synuclein (Thy1-aSyn) show enhanced tone fear.

- Alpha-synuclein pathology is overt in the basolateral nucleus of the amygdala.

- This is accompanied by microglial activation and parvalbumin neuron loss.

- Thy1-aSyn mice are useful to study mechanisms and treatment of anxiety in Parkinsons disease.

Fear Conditioning Timeline
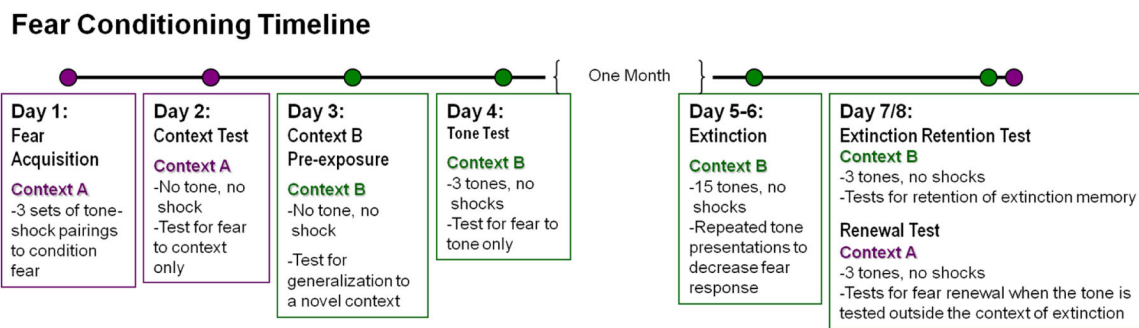
Fig. 1.

Timeline for fear conditioning and fear extinction behavioral testing. Pain sensitivity and stress-induced hyperthermia were tested after the completion of all fear testing.
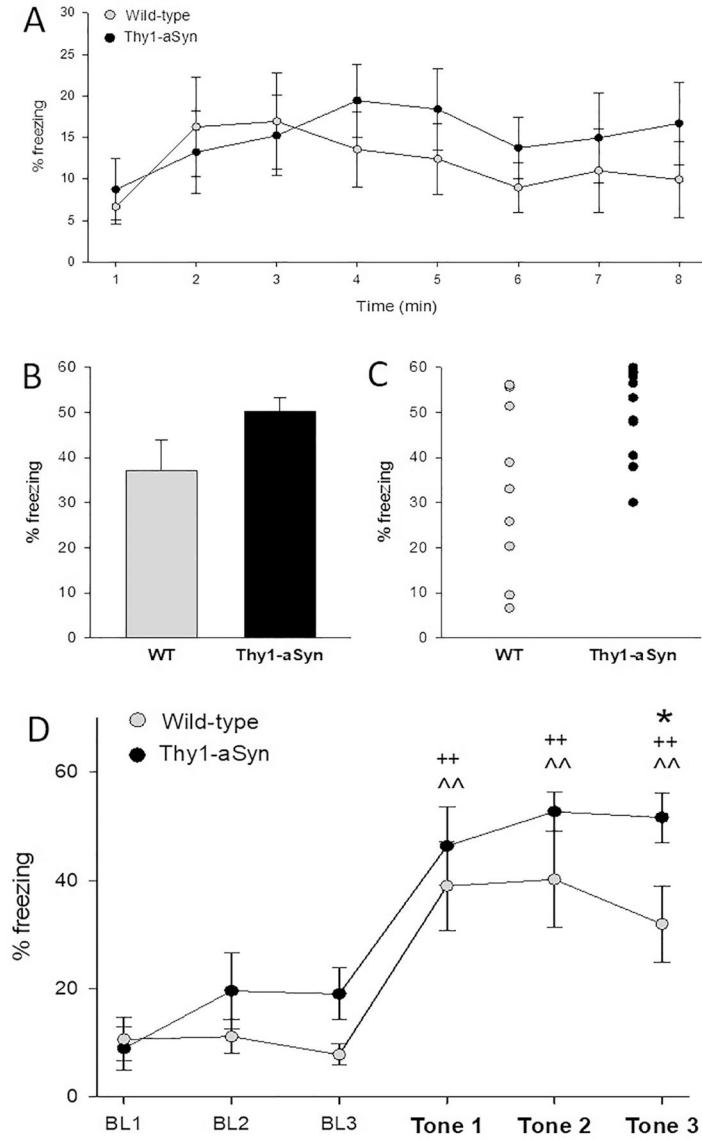
Fig. 2.

Thy1-aSyn mice (n=11) show increased freezing after conditioning in response to tone but not to context compared to wild-type (WT, n=10). A) Average freezing to context A (Day 2) across 8 minutes of context exposure (means ± SEM). Context fear is similar in Thy1-aSyn and WT mice. B) Average freezing across three tone test presentations (Day 4) (means ± SEM, p=0.088) and C) separately plotted for each mouse. Thy1-aSyn mice showed significant shift of distribution towards higher fear response (average % freezing, fisher exact test p = 0.035). D) Means ± SEM for average % freezing during the tone test. BL1–3, baseline recordings for 3 minutes without tone. Tone 1–3, recordings for 10 seconds after each tone is played. WT and Thy1-aSyn mice show enhanced average % freezing in response to the tone. (^^p<0.01 compared to BL1 for WT; ++p<0.01 compared to BL1 for Thy1-aSyn mice, Fisher's LSD). Thy1-aSyn mice showed significant increased

fear response compared to WT mice after the third tone (*p<0.05 Fisher's LSD compared to WT).
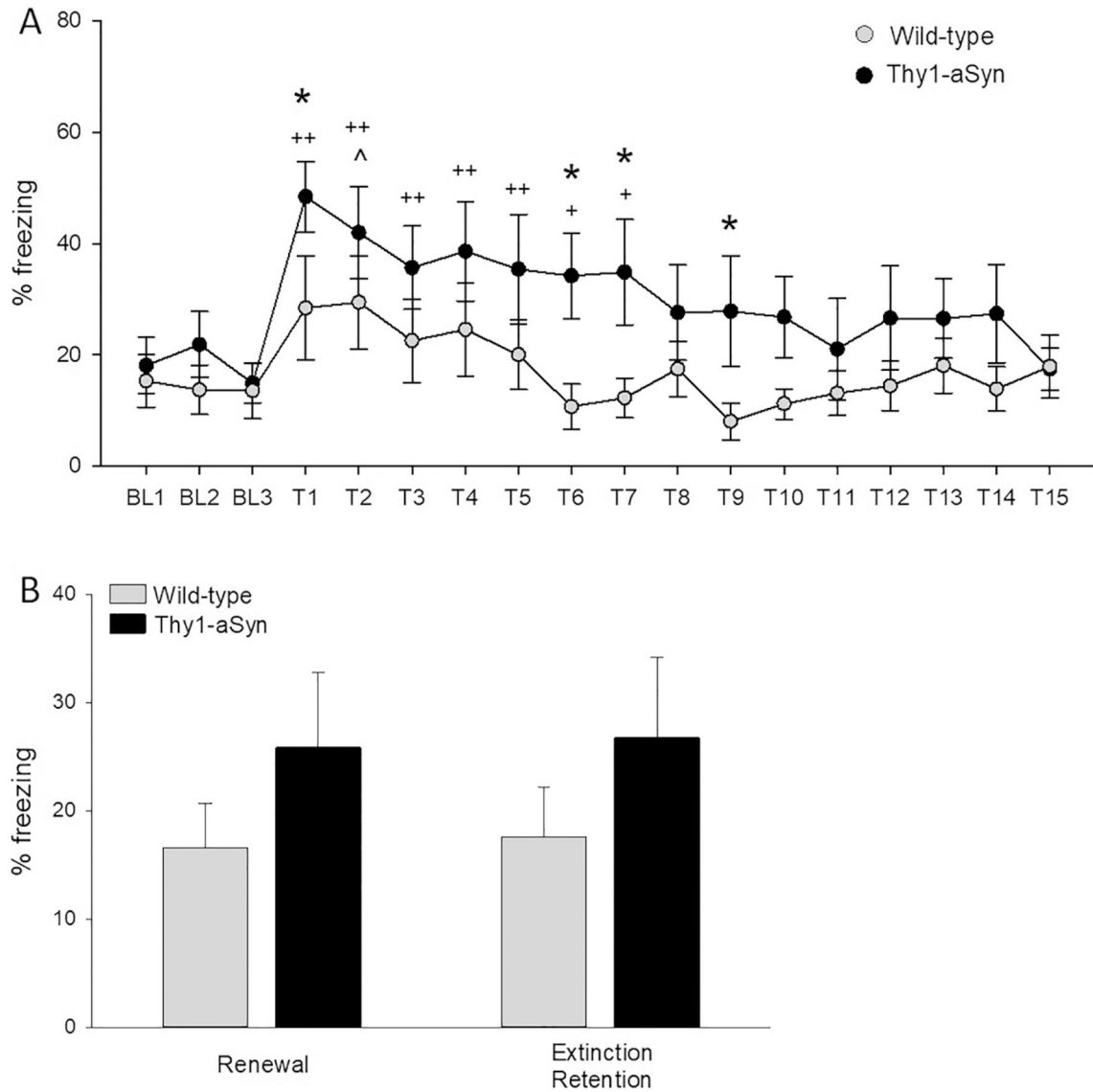
Fig. 3.
A) Higher freezing in Thy1-aSyn mice (n=11) compared to wild-type (WT, n=10) persists across extinction. Means ± SEM for average % freezing during the extinction test. BL1–3, baseline recordings for 3 minutes without tone; Tone 1–15 to extinct fear response, recordings for 10 seconds after each tone. WT mice show enhanced average % freezing in response to the tone only for T2. Thy1-aSyn mice show enhanced freezing after T1–7 before reaching extinction at T8 (^p<0.05 compared to BL1 for WT; +p<0.05,++p<0.01 compared to BL1 for Thy1-aSyn mice, Fisher's LSD). Thy1-aSyn mice showed significant increased fear response compared to WT mice after T1, T6, T7 and T9 (*p<0.05, Fisher's LSD compared to WT). B) Renewal and extinction retention of acquired fear (average freezing time to 3 tones in Thy1-aSyn and WT mice). For fear renewal mice were placed back in context where fear was acquired (but not extinguished). For extinction retention mice were placed back in context where fear was extinguished (mean ± SEM, 2×2 RM ANOVA n.s.).
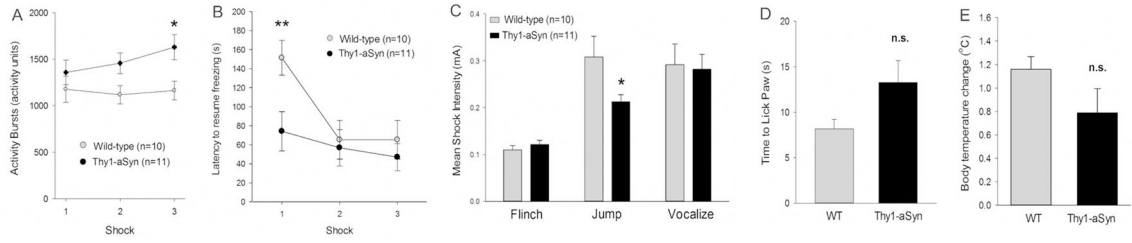
Fig. 4.

Responsiveness to foot shocks, stress and pain A) Increased activity burst immediately after the third shock during fear acquisition in Thy1-aSyn mice (n=11) compared to wild-type (WT, n=10) (*p < 0.05, post hoc, mean ± SEM) B) Thy1-aSyn mice need less time to resume freezing after receiving the first shock (**p < 0.01, post hoc, mean ± SEM). C) Thy1-aSyn mice respond with jumps at lower shock intensity compared to WT, but flinch and vocalize at similar intensities (*p < 0.05, Fisher's LSD, mean ± SEM). D) Thy1-aSyn take do not show more sensitivity compared to WT on a hot plate measured by time to lick the paw in response to heat (WT: n=5, Thy1-aSyn: n=9, mean ± SEM, Student's t-test ns). E) Thy1-aSyn mice respond with similar body temperature increase after repeated stress compared to WT (WT: n=5, Thy1-aSyn: n=9, mean ± SEM, Student's t-test ns).
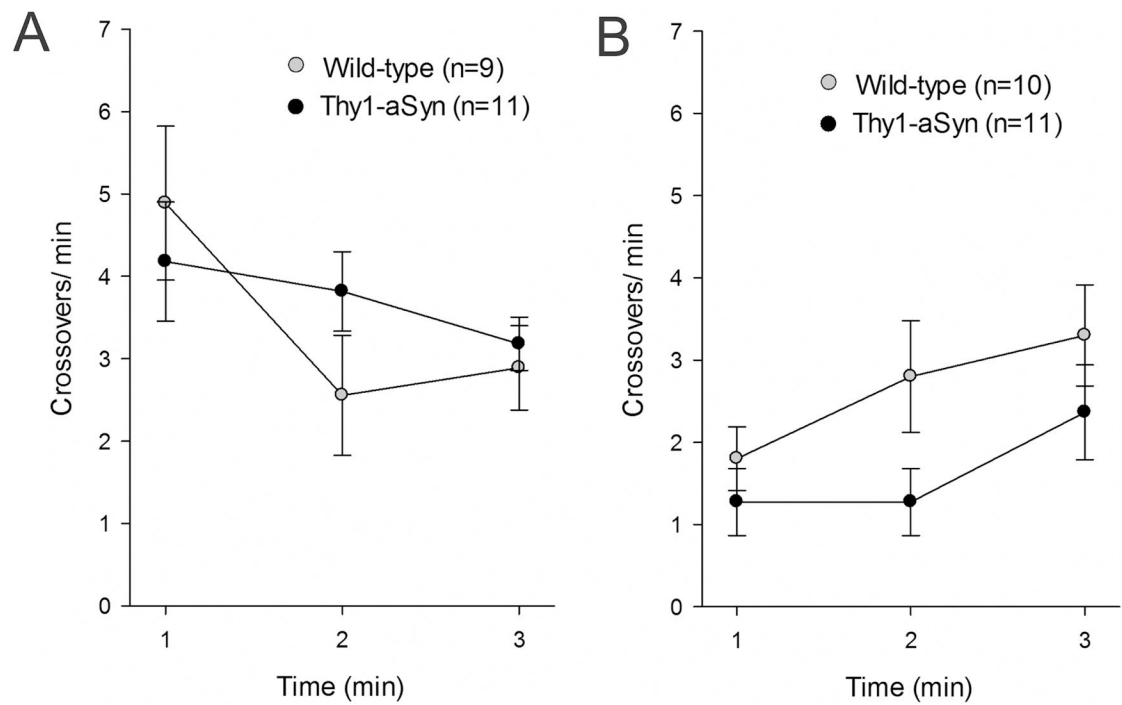
Fig. 5.
No differences in crossovers during fear conditioning. A) Crossovers during the first three baseline minutes of fear acquisition in context A; no significant difference between wild-type (WT, n=9–10) and Thy1-aSyn mice (n= 11, means ± SEM) B) General activity during the first three baseline minutes of the tone test in context B; no significant difference between WT and Thy1-aSyn mice (means ± SEM, 2X3 RM ANOVA ns).
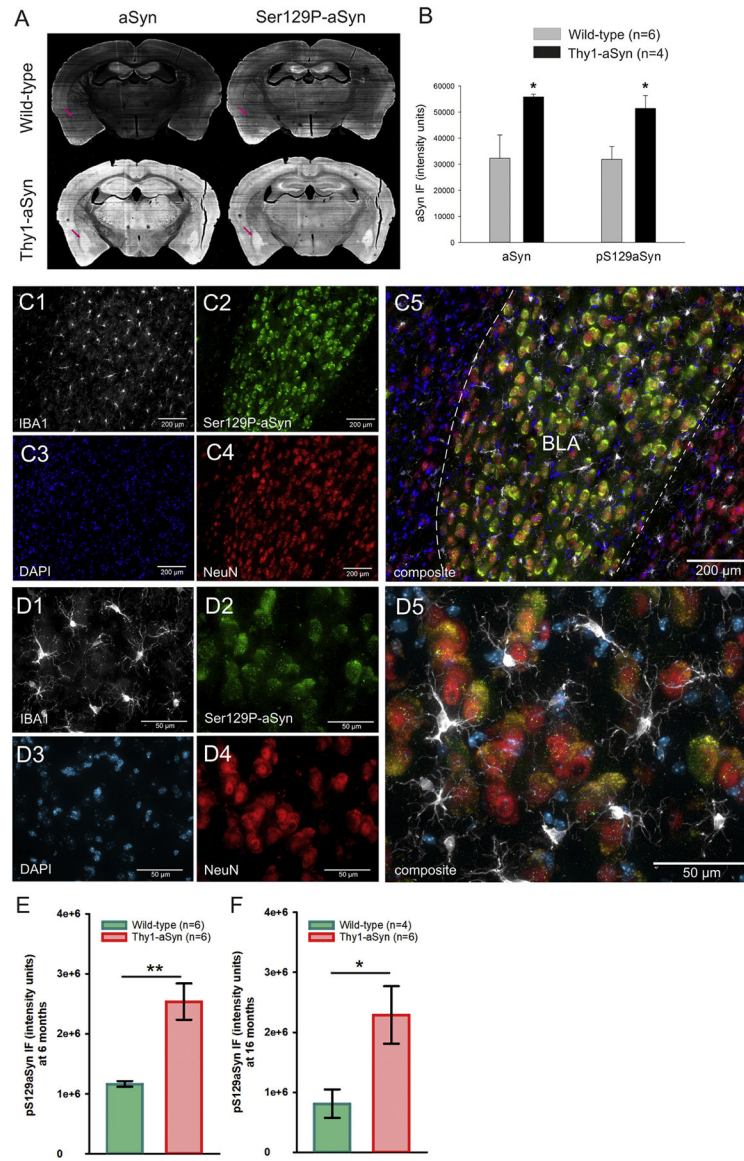
Fig. 6.
Immunofluorescent staining of human and mouse α-syn and phosphorylated α-syn (Ser129P-α-syn) antibodies in sections of the amygdala. A,B) Thy1-aSyn transgenic mice extensively accumulate aSyn and Ser129P-aSyn in the amygdala (purple arrow, mean + SEM, Student's t-test; $*p < 0.05$). C, D) Thy1-aSyn transgenic mouse with accumulated Ser129P-aSyn in the BLA at two magnifications. Phosphorylated α-syn accumulation (C2, D2) was apparent in NeuN positive cells (C4, D4), but not all NeuN positive cells contained Ser129P-aSyn; IBA-1 positive cells (C1, D1) and a number of DAPI stained cells (C3, D3) appear devoid of Ser129P-aSyn. IBA-1 positive cells (C1, D1) appear with enlarged cell bodies and activated morphology. Basolateral nucleus of the amygdala (BLA), scale bar = 200 μm (C) or 50 μm (D). E, F Quantification of Ser129P-aSyn accumulation in the BLA of 6 months old (E) and 16 months old (F) mice (mean ± SEM, Student's t-test; $*,**p < 0.05$, 0.01, N is provided in figure).
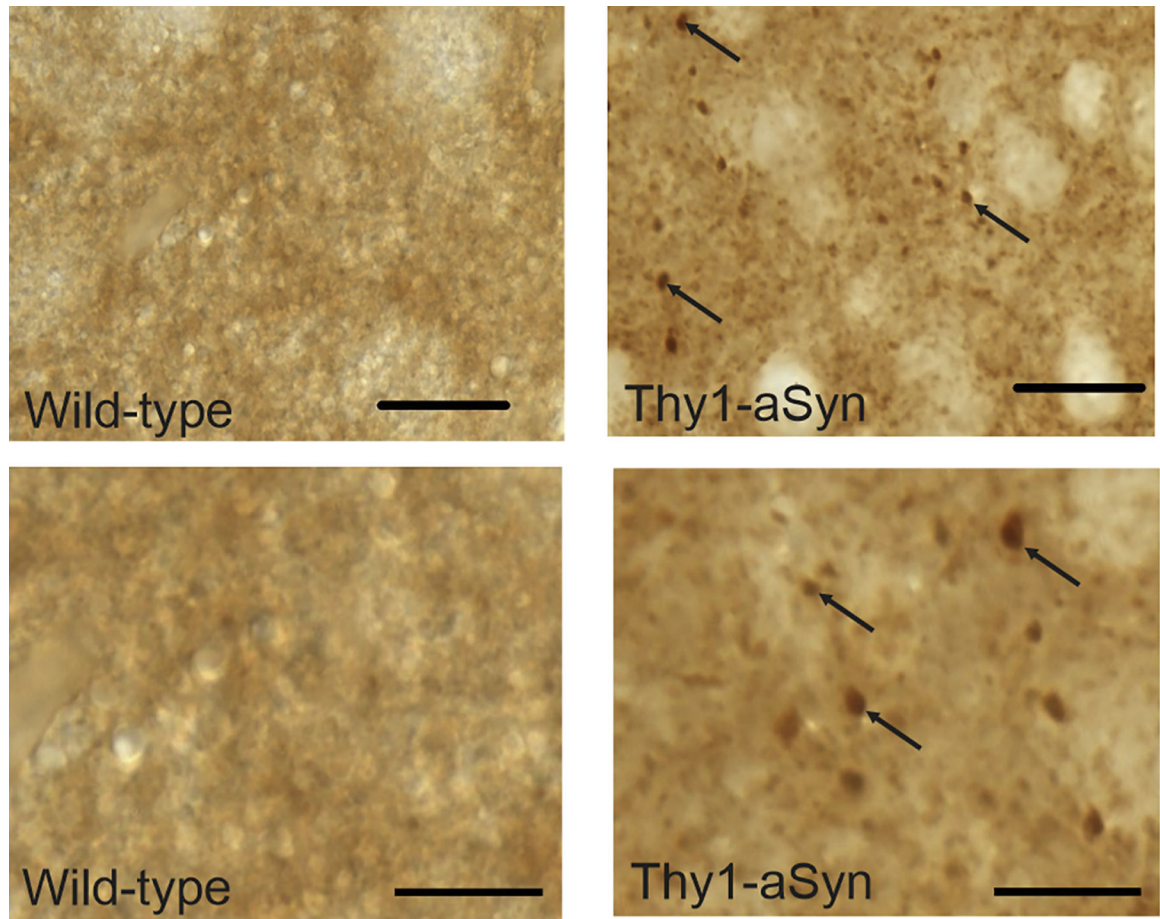
Fig. 7.
Alpha-syn positive proteinase K-resistant aggregates in coronal sections of the basolateral nucleus of the amygdala of Thy1-aSyn transgenic mice (black arrows, lower panel shows higher magnification). No aggregates were detected in wild-type mice. Scale bar 20 μm upper panel, 10 μm lower panel.
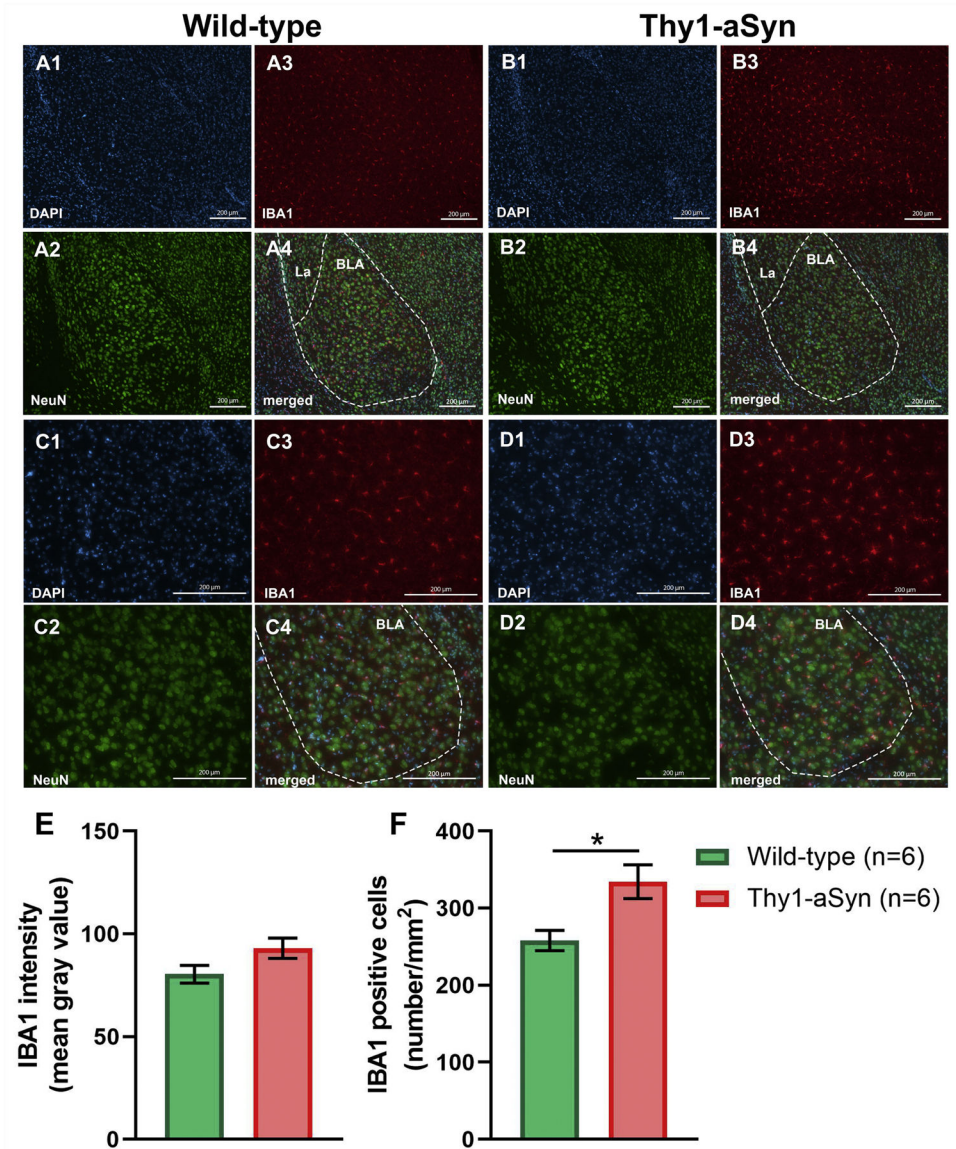
Fig. 8.

Immunofluorescent (IF) NeuN and IBA-1 staining of amygdala sections from wild-type (WT) and Thy1-aSyn (TG) mice. Representative IF microphotographs of DAPI (blue), NeuN (green), IBA-1 (red) and merged IF images of the 6-months WT (A, C) and TG mice (B, D). Representative (10×) IF images (A, B) of basolateral nucleus of the amygdala (BLA). Representative (20×) IF images of BLA (C, D). Image-J was used to quantify the IF intensity of IBA-1 staining and density IBA-1 positive cells. Change in expression of IBA-1 (E) was not observed between experimental groups. Increased density of IBA-1 positive cells was observed in TG mice compared to WT mice (F). (mean ± SEM, $n = 6$/group; Student's t-test; *$p < 0.05$) Lateral amygdaloid nuclei (La), scale bar = 200 μm.
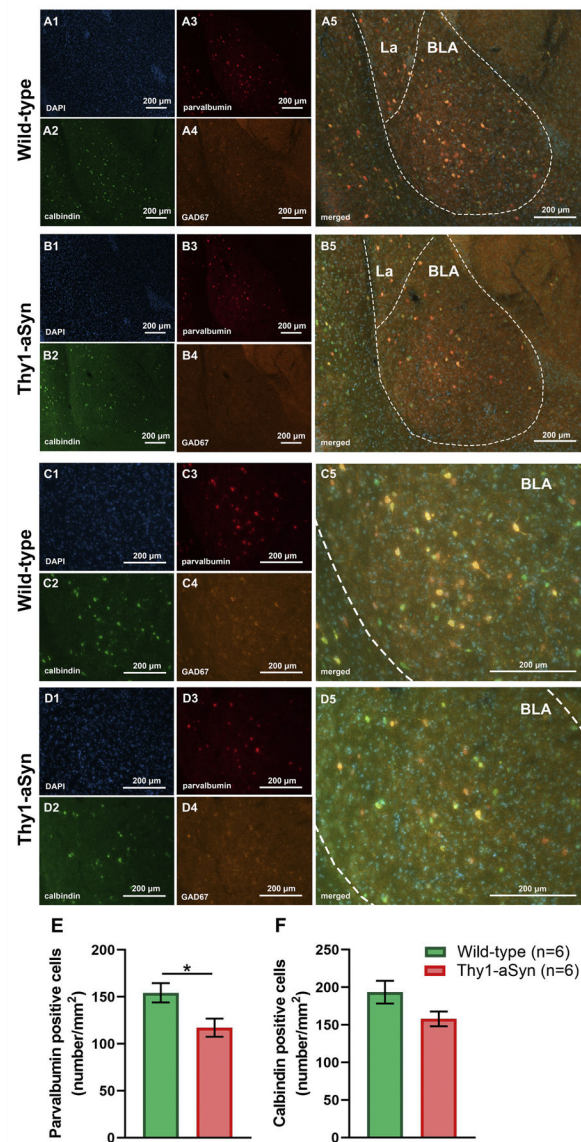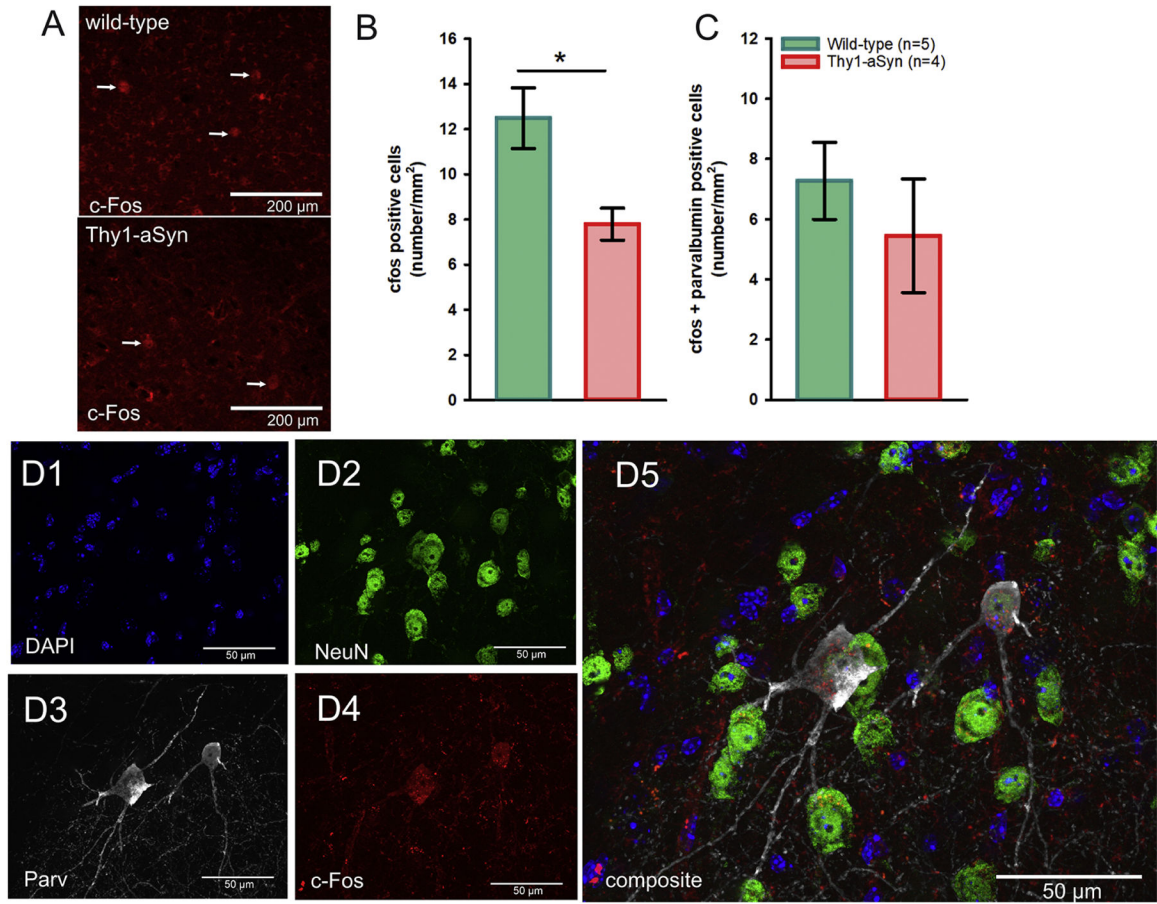
Fig. 9.

Immunofluorescent (IF) calbindin, parvalbumin and GAD67 staining of amygdala sections from wild-type (WT) and Thy1-aSyn (TG) mice. Representative IF microphotographs of DAPI (blue), calbindin (green), GAD67 (orange), parvalbumin (red) and merged IF images of the 6-mo WT (A, C) and TG mice (B, D). Representative (10×) IF images (A, B) of basolateral nucleus of the amygdala (BLA). Representative (20×) IF images of BLA (C, D). Reduction of parvalbumin but not calbindin positive cell density was observed in TG mice compared to WT mice (E, F). (mean ± SEM, n = 6/group; Student's t-test; *p < 0.05) Lateral amygdaloid nuclei (La), scale bar = 200 μm.

Fig. 10.
Immunofluorescent (IF) c-Fos staining of amygdala sections from wild-type and Thy1-aSyn mice. A) Representative IF microphotographs of c-Fos positive cells in wild-type and Thy1-aSyn mice (white arrows), B) Quantification of c-Fos positive and C) c-Fos/Parv double-positive cells in the BLA (mean ± SEM, Student's t-test; *p < 0.05, N is given in the bar graph). D1–5) DAPI (blue), NeuN (green), parvalbumin (Parv, grey), c-Fos (red) and merged images of the BLA from a representative Thy1-aSyn mouse demonstrates c-Fos and parvalbumin co-localization (scale bar = 50 μm).